Energy Trading in Local Electricity Markets With Behind-the-Meter Solar and Energy Storage

Li He, *Member, IEEE*, and Jie Zhang, *Senior Member, IEEE*

***Abstract*—Distributed energy resources, especially residential behind-the-meter photovoltaics (BTM PV), have been playing increasingly important roles in modern smart grids. Residential net-load, which is closely tied with customers' gross load consumption and weather, is usually the only data available for the market operator in a local electricity market (LEM). This paper seeks to design customized prices for an LEM that consists of an agent, BTM PV, energy storage (ES), prosumers, and consumers. The LEM agent who owns a community-scale ES system is responsible for operating the market, determining the internal price, and facilitating the energy sharing within the community. A hierarchical energy trading infrastructure is considered, where the LEM agent acts as the mediator between the external utility grid and customers. A two-stage decision-making framework, including both look-ahead ES scheduling and real-time customized price design, is developed for the agent's profit maximization. Besides, the impacts of netload forecasting and BTM PV disaggregation are also investigated. The customer's consumption behavior is modeled as a utility maximization problem. Compared with the benchmark uniform price design, it is found that the customized pricing scheme could further improve the LEM agent's profit by 4% to 130%, depending on the weather conditions and seasonal load patterns.**

***Index Terms*—Behind-the-meter solar, customized price design, energy sharing, energy storage, local electricity market.**

I. Introduction

With the increasing penetration of distributed energy resources (DERs) over the past decade, such as behind-the-meter (BTM) rooftop photovoltaic (PV) panels, electricity markets are undergoing a significant transition, from traditional centralized management to a decentralized, bottom-up, and localized framework. The fast-growing installation of solar panels creates a potential to feed massive negawatt power [1] back into the grid, raising unexpected challenges to power system reliability. Community solar [2] has shown to be an innovative local electricity market (LEM) to address this challenge, which is gaining popularity across the U.S. in recent years. Allowing neighbors to share their excess PV generation, unused energy storage (ES) capacity, and spare roof space, etc., this novel transactive business mode could benefit prosumers, consumers, and power grids by reducing the local community's reliance on the utility grid, fully utilizing customers' flexibility to participate in demand response (DR), achieving a better generation-load balance, and mitigating unexpected energy crises.

Extensive explorations have been conducted on designing and evaluating peer-to-peer (P2P) markets, LEM and demand-side management, among which game theory has been widely used to address the interaction between different stakeholders. For example, a Nash equilibrium-based game-theoretic approach has been used to validate how energy is traded among peers within a microgrid or community during the bidding process [3], [4]. A leader-follower game [5], [6], [7] has been used to model the interaction between the market agent and customers, since a trustful third-party stakeholder like an agent is needed to manage and allocate the LEM and supply local customers. In addition to non-cooperative games, in order to understand the potential cooperative behaviours between multiple participants in an LEM, a cooperative game has also become a prevailing approach that focuses on predicting which coalitions to form, what joint actions the groups should take, and the resulting collective payoffs. For example, Refs. [8], [9], [10] used cooperative games to determine how to share PV and ES with cooperators. Besides, Paudel et al. [11] proposed different game-theoretic models for P2P trading among prosumers and consumers, such as a non-cooperative game among sellers, an evolutionary game of buyers selection, and a Stackelberg game between buyers and sellers.

In addition to game-theoretic approaches, many other methods have also shown to be effective to address the pricing and demand-side management problem in LEM. For example, auctions [12], [13] are a common method to involve both buyers and sellers to clear the market. A continuous double auction was introduced in [14], which focused on a prediction-integration adaptive bidding strategy that all prosumers and consumers can perform informed trading. Guerrero et al. [15] proposed a decentralized P2P energy trading platform based on a continuous double auction considering a physical low-voltage network constraint, where agents with zero intelligence plus bidding strategies were considered. Other methods such as machine learning-based decision-making [16], [17], model predictive control [18], dynamic programming [19] etc. have also been explored in LEM.

Manuscript received 13 September 2022; revised 15 January 2023; accepted 19 February 2023. Date of publication 1 March 2023; date of current version 15 June 2023. Paper no. TEMPR-00037-2022. *(Corresponding author: Jie Zhang.)*

Li He is with the Department of Electrical and Computer Engineering, The University of Texas at Dallas, Richardson, TX 75080 USA (e-mail: li.he@utdallas.edu).

Jie Zhang is with the Department of Mechanical Engineering and (Affiliated) Department of Electrical and Computer Engineering, The University of Texas at Dallas, Richardson, TX 75080 USA (e-mail: jiezhang@utdallas.edu).

Digital Object Identifier 10.1109/TEMPR.2023.3250948

Most of the methods mentioned above mainly focus on the design of a unique price, i.e., a uniform pricing rate is applied to all customers. In a realistic retail market, however, residential customers have different daily routines and consumption preferences, and price discrimination [20] for customers has recently been explored in the market design, especially in deregulated energy markets. For example, utility companies have already offered customers different energy plans, such as flat rate, time-of-use (ToU), real-time price (RTP), discriminated price, reimbursed renewable, free night/weekend, feed-in tariff (FiT) [21], etc. It is found from the literature that the pricing model plays a crucial role in an LEM, which directly impacts the participants' incentives of price-based DR. However, there still exist research gaps in the existing literature that need to be bridged.

Although accurate forecasting is desired in system operations, even with state-of-the-art forecasting models, the errors still exist in both demand and generation sides. To manage the uncertainty in both transactive and non-transactive markets, methods such as two-stage optimization [16], [22] and energy storage (ES) scheduling [7], [23] have been explored in the literature. Some existing works have also shown the effectiveness of multi-stage energy dispatches, e.g., Ref. [24] helps the market operator to adaptively incorporate the real-time observations into the dataset and update future decision-making to mitigate the forecasting uncertainty. Besides, the correlation among the agents within the LEM could also be leveraged to improve the forecasting accuracy and promote the profitability, since local customers might share similar solar power generation profiles and daily consumption patterns. In addition, the real-time updated information in the market could also be leveraged to improve the future decision-making.

This study is a more comprehensive extension of our previous work presented in [25]. In our earlier work, we simply assume that the agent has perfect information of customers' load, PV power generation, and consumption preferences. While in the current study, a deep learning model is leveraged to forecast customers load and PV power generation, which is more reasonable and practical. The study herein provides an alternative method to estimate the consumption flexibility of the customer for cases where only the aggregated netload is available, while the BTM PV installation and generation is invisible. Two main research gaps still exist in effective pricing schemes before LEMs (with high DER penetration) could be widely established. First, it is important to consider a number of critical factors in the pricing strategy of an LEM, such as the energy sharing ability, demand management flexibility, BTM solar capacity of different customers, and robustness to uncertainties. Second, although BTM solar forecasting and BTM disaggregation have been extensively studied with flourishing smart meter data and advancement in machine learning, there still exist research gaps on how to leverage the forecasting and disaggregation results in market operations. Effective and accessible forecasting and disaggregation models without relying heavily on challenging-to-obtain data and private information are desired. To address these challenges and bridge the research gap, the main contributions of this paper could be summarized as:

1) A multi-input single-output (MISO) LSTM model is leveraged for improving the forecasting accuracy, by which the spatial relationships between different households and the community are indirectly considered. Customers' BTM solar generation and gross consumption patterns are disaggregated to analyze their consumption preferences and load flexibility. A price discrimination scheme is developed to fully incentivize flexible customers to consent to the maximum energy sharing flexibility.
2) A two-stage decision-making framework for the LEM agent, including both the look-ahead ES scheduling and real-time scheduling updating, is developed. Specifically, stage one is modeled as a cost minimization problem using the aggregated netload forecasts to optimize the ES scheduling, with the aim of mitigating the negawatt fed back to the grid. Stage two is modeled as a revenue maximization problem to further improve the customers' energy management and the LEM agent's profit.

The rest of the paper is organized as follows. Section II describes the proposed LEM, consisting of agent's ES scheduling, customized price design, and customer consumption models. Section III describes the netload forecasting and BTM PV disaggregation methods. Section IV shows a case study with 10 customers to evaluate the performance of the LEM price design. Concluding remarks and future work are discussed in Section V.

II. Overall LEM Framework and Methodology

The overall structure of the proposed LEM is introduced in this Section. The LEM consists of an agent (who owns a community-scale ES system) and $\mathcal{N}$ energy sharing customers (including $\mathcal{N}_p$ prosumers with BTM PV panels and $\mathcal{N}_c$ pure consumers, $\mathcal{N}_p \cup \mathcal{N}_c = \mathcal{N}$). Each customer can only act as either a buyer $\mathcal{N}_b$ or a seller $\mathcal{N}_s$ at one time, similarly, $\mathcal{N}_b \cup \mathcal{N}_s = \mathcal{N}$. The market works in an agent-based trading mode: the market agent trades with all customers with internal customized prices; besides, the market agent is also responsible for balancing the supply and demand in the LEM with the external grid under utility prices (i.e., ToU and FiT prices in this work). The agent possesses a centralized ES at the aim of mitigating the over-generation PV of the community.

A. Decision-Making Process

The LEM decision-making consists of two major steps: look-ahead ES scheduling and real-time prices design, which are briefly described as follows.

1) *Stage 1 – Look-ahead ES scheduling:* The LEM agent first determines the ES capacity scheduling based on the aggregated netload of the community to promote the self-consumption of solar generation and maximize its profit.

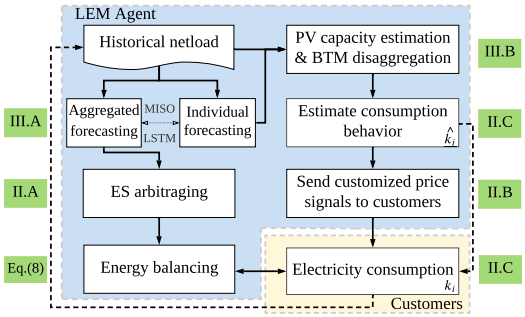

Fig. 1. Hierarchical decision-making for the LEM agent and customers.

Since the state of charge (SoC) of ES is time-coupled, it is more reasonable to determine the ES scheduling in a look-ahead manner.

2) *Stage 2 – Real-time customized price design:* The LEM agent designs customized pricing schemes for different customers to fully incentivize the customers' sharing elasticity. The agent and customers are assumed to act rationally and strategically to pursue their own interests, i.e., maximizing their profit/utilities in this work. Since the trading in LEM occurs in each hour, the customized price design and energy consumption occur in a real-time manner.

In this two-stage framework, the agent decides the ES scheduling in a look-ahead manner. Otherwise, the ES schedules would completely depend on the current information. For example, the agent may fully discharge ES when the PV output is limited if it failed to forecast an upcoming price hike, however, it is more economical to discharge the buffered energy in the subsequent time slots. Besides, with the two-stage framework, the forecasting accuracy could be further improved with shorter lead time and more information the agent could obtain as the market operates. The overall process of two-stage decision-making for the LEM agent and customers is illustrated in Fig. 1, by connecting the components and models to be introduced in Sections II and III.

B. ES Capacity Scheduling

The primary goal of the LEM agent's ES scheduling is to promote renewable consumption and mitigate negawatt power in the LEM. The objective function of the agent is modeled as minimizing the trading cost C with the external utility grid, since the energy sharing within the LEM (i.e., from prosumers to buyers) does not impact the aggregated netload of the LEM.

$$\min C = \sum_{t=h}^{H} \left[\pi_s^t \left(NL^t + x^t, 0 \right)^+ + \pi_f^t \left(NL^t + x^t, 0 \right)^- \right] \tag{1}$$

$$NL^t = \sum_{i=1}^{\mathcal{N}} (l_i^t - p_i^t) \tag{2}$$

$$-\Lambda \cdot C_{rate} \le x^t \le \Lambda \cdot C_{rate} \tag{3}$$

$$SoC_{\min} \le SoC^t \le SoC_{\max} \tag{4}$$

$$SoC^t = \begin{cases} SoC^{t-1} + x^t \cdot \eta, & x_i^t > 0 \\ SoC^{t-1} + x^t / \eta, & x_i^t < 0 \end{cases} \tag{5}$$

We define $(\cdot)^+ = \max(\cdot, 0)$, and $(\cdot)^- = \min(\cdot, 0)$. The parameter H is the optimization window (i.e., 24 h), and h is the current time slot. The parameter C denotes the trading cost with the utility grid from the current time h to future H. The parameter NL^t denotes the aggregated netload of the community at time t, which is load minus PV generation in this work. The parameters l and p stand for the gross load and BTM PV generation, respectively, and the subscript i denotes the index of customer. The parameter x^t represents the battery charging/discharging schedule, and η is the (dis-)charging efficiency. The parameter Λ is nominal capacity of the ES. The terms of $-\Lambda/C_{rate}$ and Λ/C_{rate} are the lower and upper bounds of the (dis-)charging energy in each time slot, respectively, and C_{rate} is the maximum (dis-)charge rate of the ES. The parameter SoC^t is the SoC of the ES at the end of time slot t; SoC_{min} and SoC_{max} are the lower and upper limits of the ES, respectively.

C. Agent's Customized Prices Design

In a deregulated electricity market, customers are allowed to freely choose their desired pricing schemes. Building upon this, a customized price design framework is further proposed to fully incentivize customers' flexibility in energy sharing. If consumers act rationally and strategically to pursue their own self-interest, i.e., maximizing their utilities in this work, then the problem falls squarely in the realm of game theory, and in particular, choose the best action by responding to different prices designed by the retailer. A successful price-based DR program should be designed to attract the interest of customers to participate in, through the provision of incentives to impact their original behaviour while at the same time minimizing their discomfort. To make the customized prices attractive, the LEM agent should ensure that the customers gain more benefits compared with the previous pricing scheme. In this way, consumers are willing to accept the customized price, since they can achieve higher utilities or lower costs with the customized price. In this work, the following constraint is implemented as:[1]

$$\pi_f \le \lambda_b \le \lambda_s \le \pi_s \tag{6}$$

The buying prices λ_b refer to the solar buy-back rate for sellers $\mathcal{N}_s$, while the selling prices λ_s refer to the energy charge for buyers $\mathcal{N}_b$, and $\lambda_b < \lambda_s$ is to ensure the agent's profit. Besides, λ_b and λ_s prices are constrained by the utility price, i.e., the FiT (π_f) and ToU (π_s).

[1]It should be noted that the prices and consumption hold $\forall t \in [h, H]$ for (2)–(12), and the superscript t of all time-dependent parameters is omitted in (6)–(12).

Based on the discussion above, the real-time profit maximization of the customized prices design is formulated as:

$$\max P = \begin{cases} \sum \boldsymbol{\lambda_s} \odot \boldsymbol{E_b} - \sum \boldsymbol{\lambda_b} \odot \boldsymbol{E_s} - \pi_s \Delta E, & \Delta E \geq 0 \\ \sum \boldsymbol{\lambda_s} \odot \boldsymbol{E_b} - \sum \boldsymbol{\lambda_b} \odot \boldsymbol{E_s} - \pi_f \Delta E, & \Delta E < 0 \end{cases} \tag{7}$$

where $\boldsymbol{E_b}$ and $\boldsymbol{E_s}$ denote the total demand set from buyers $\{[l_i - p_i], i = 1 : \mathcal{N}_b\}$ and supply set from sellers $\{[p_i - l_i], i = 1 : \mathcal{N}_s\}$ inside the community, respectively. The parameters $\boldsymbol{\lambda_s}$ and $\boldsymbol{\lambda_b}$ denote customized prices set for buyers and sellers, respectively. The parameter ΔE denotes the imbalance between supply and demand, which is defined as:

$$\Delta E = \sum \boldsymbol{E_b} - \sum \boldsymbol{E_s} + x \tag{8}$$

The imbalance needs to be mitigated with the utility grid, and x is a known number which is already obtained from (1). A positive ΔE denotes that the agent has to purchase power, and a negative value denotes feeding negawatt back to the grid. Since the ground truth $\boldsymbol{E_b}$ and $\boldsymbol{E_s}$, including individual l_i and p_i, are not available for the LEM agent, the customized prices are determined based on the netload forecasts and disaggregation, which will be introduced in Section III.

D. Customers Consumption Model

In this work, all customers are assumed to act rationally and strategically to pursue their own interest, i.e., aiming to find an optimum gross consumption scheduling (l) by responding to different prices (λ) across a predefined optimization window H. The customers' objective could be to minimize the daily cost [3], [8], minimize the inconvenience of DR [26], or maximize the satisfaction level of consumption [7]. In this paper, the utility function from [16] is adopted, which describes the customers' consumption preferences as two parts: the satisfaction from consuming energy and the cost of trading energy.

$$\max\ U_i = \begin{cases} k_i \ln(1 + l_i) - \lambda_s (l_i - p_i), & l_i \geq pv_i \\ k_i \ln(1 + l_i) - \lambda_b (l_i - p_i), & l_i < pv_i \end{cases} \tag{9}$$

For consumers, $p = 0$. In (9), $k_i \ln(1 + l_i)$ is the utility achieved by the customer i through consuming energy l. The logarithm $\ln(\cdot)$ function has been widely used in economics for modeling the preference of users due to its close relation to fair DR [7]. And $(1 + \bullet)$ is a typical modified form to avoid $-\infty$. A greater value of k indicates a higher consumption willingness. Besides, it is derived from (9) that a higher selling price λ_s will result in a higher consumption for a buyer ($l_i \geq pv_i$), while a higher buying price λ_b will encourage a seller ($l_i < pv_i$) to trade more energy by adjusting consumption.

To solve (9), we find that the customers' decision variables (l) are dependent on the prices (λ) designed by the market agent. Thus for any given price λ_b or λ_s at each hour, the customer i will adapt its optimal consumption l_i^* as the best response to λ for maximizing its utility U_i, which is calculated as:

$$\begin{aligned} l_i^* &= \arg\max\ U_i(k_i, l_i, pv_i, \lambda_b, \lambda_s) \\ &= \begin{cases} k_i/\lambda_s - 1, & l_i \geq pv_i \\ k_i/\lambda_b - 1, & l_i < pv_i \end{cases} \end{aligned} \tag{10}$$

As for the consumption preference parameter k, we consider two different values, namely, i) the ground-truth k, which remains as private information and is only accessible to customers themselves, and ii) the estimated $\hat{k}$, which is the agent's inferred value based on the estimation. For example, in Refs. [27], [28], the price-consumption response data was leveraged to estimate the consumers' preference. In this work, the customer's ground-truth k is calculated based on the original gross load and the utility prices (i.e., ToU and FiT). Specifically, the customers are assumed to have adapted their original gross consumption as the best response to the original pricing scheme [29]. And the private ground-truth k of customer is obtained by reverse-engineering (10) with its real gross load, PV generation, and utility prices, which is calculated as:

$$k_i = \begin{cases} \lambda_s (l_i^* + 1), & l_i \geq pv_i \\ \lambda_b (l_i^* + 1), & l_i < pv_i \end{cases} \tag{11}$$

However, customers' real load and PV generation data are not available to the agent, and the agent needs to disaggregate the gross load and PV generation via the only accessible data, i.e., netload, which will be introduced in the next section.

If a customer's behavioural characteristics, together with the appliance identification, could be obtained, then the customer's residential daily patterns could be leveraged for more accurate DR modeling. In this work, the appliances information is not available due to limited data availability. To streamline the model, the following constraint has been added to the gross load.

$$l_i \in [l_{min}, l_{max}] \tag{12}$$

where $[l_{min}^h, l_{max}^h]$ is the range of customer i's electricity consumption, which can be extracted from historical usage.

Convergence Analysis: The optimal solution obtained from (10) holds when it is located within the consumption constraint (12). Otherwise, the optimal solution l_i^* will always lie on the boundary due to its strict concavity. Thus, each customer has an existing and unique best response to any price designed by the agent. Besides, there are no coupled constraints between customers, thus each customer's response is independent with others. By substituting (10) into (7), the Hessian matrix of P is negative definite, thus there also exists a maximum profit in a bounded region $[\pi_f, \pi_s]$, indicating that the agent has an a unique pricing strategy to maximize its profit. A similar proof process could be found in Ref [7], where the authors proposed to prove the existence and uniqueness of the Stackelberg Equilibrium.

III. Netload Forecasting and BTM PV Disaggregation

In the previous section, we introduced the customers' consumption model. However, since customers' gross load l and

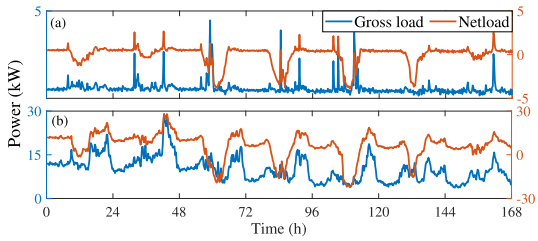

Fig. 2. Gross load and netload curves of (a) 1 customer, and (b) 10 customers in a week.

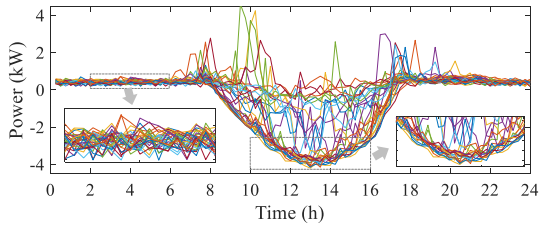

Fig. 3. Netload curves of prosumer 1 in January 2018.

BTM PV data p in (9) are unavailable to the retailer, it is challenging to accurately analyse the customers' ground-truth gross consumption behaviors. To address this challenge, we propose to disaggregate the only accessible data (i.e., netload) into BTM PV generation and gross load. Since the solar generation p cannot be used for DR, the consumption flexibility only derives from the gross load. We first propose a forecasting-assisted pricing model that could help the LEM agent to predict the aggregated as well as individual netload in the market. Then we use the historical netload dataset to estimate the maximum generation and then disaggregate the netload into BTM PV generation and gross load. After disaggregation, the $\hat{k}$ is calculated by reverse-engineering (9), then the customized price for individual household is determined.

A. Long Short-Term Memory Netload Forecasting

Long short-term memory (LSTM) is an artificial recurrent neural network architecture with feedback connections, which is capable of processing single data points as well as entire data sequences. To better capture the temporal dependencies of a time series, LSTM introduces different gates which could regulate the gradient flow of the network. Such characteristic is ideal for load forecasting since the customers' consumption has been proven to follow certain routines due to strong temporal relations. A common LSTM unit is composed of a memory cell $\mathbf{c}$, an input gate $\mathbf{i}$, an output gate $\mathbf{o}$, and a forget gate $\mathbf{f}$. The cell remembers values over arbitrary time intervals and the three gates regulate the flow of information into and out of the cell. The detailed LSTM formulations could be found in [30].

The aforementioned traditional LSTM is also referred to the traditional single-input single-output (SISO) model, which means only time-series load consumption of the selected household is used as input to predict its future load. Only temporal dependencies are consider in the SISO model. This paper adopts a multi-input single-output (MISO) LSTM [31] for netload forecasting, by which the spatial relationships between different households within the LEM and the community aggregated netload are indirectly considered. Fig. 2 presents the gross load and netload curves of 1 customer and the aggregation of 10 customers. It can be seen that the BTM PV has a significant impact on the netload curves, which makes it a duck curve. Due to customers' various consumption behaviors, it is challenging to accurately forecast individual gross load, as shown in Fig. 2(a). However, such volatility can be mitigated by aggregated forecasting, since the aggregated curve is smoother and more stable compared with individual curves, as shown in Fig. 2(b).

In this work, the individual and aggregated netload are generated separately. The reason to separate two different forecasts is that the agent needs more accurate aggregated netload forecasts to determine the look-ahead capacity scheduling of the centralized ES. Besides, individual netload is also desired to design customized price for each customer. More precisely, in this work each individual customer's netload forecasts are generated in parallel using the aforementioned SISO LSTM model without additional input from peers, due to various consumption behaviors and weak correlations. To improve the forecasting accuracy of the aggregated netload, historical netload profiles of additional household are simultaneously fed into the MISO LSTM model. The normalized Root Mean Square Error (nRMSE) is calculated to evaluate the accuracy of the proposed netload forecasting.

$$nRMSE = \frac{1}{y_{\max} - y_{\min}} \sqrt{\frac{\sum_{k=1}^{n} \left(\hat{y}_k - y_k\right)^2}{n}} \tag{13}$$

where $\hat{y}_k$ and y_k denote the forecasted netload and actual netload, respectively, and n denotes the number of data points. The normalization is based on the difference between the maximum and minimum values.

B. BTM PV & Gross Load Disaggregation

The essential reason of BTM disaggregation is that the netload is the only data that the LEM agent can collect from customers. BTM disaggregation can improve the accuracy of gross consumption behavior analysis of customers with inaccessible BTM PV generation data. Fig. 3 shows a typical prosumer's netload curves in a month. There are three prerequisites in estimating the BTM PV generation by only leveraging the historical netload curves.

1) The netload curves contain consumption noises due to some periodic appliances (e.g., router, freezer, and refrigerator) in the household.
2) The gross consumption never drops to zero, thus there exists a power floor for the netload curve, which occurs in an unoccupied case or no activities.
3) The observed negative netload should never exceed the maximum clear-sky PV generation.

Specifically, we propose to leverage a method that only requires the historical netload data and a *standardized* PV generation fraction p_{std} by following [32]. In a community, the neighbors with PV panels show similar output trends due to strong spatial correlations while only vary in the multitude. And those un-monitored BTM PV generation can be estimated by:

$$p_i = p_{std} \cdot G_{max.i} \tag{14}$$

where p_{std} is the monitored *standardized* PV generation and G_{max} is the estimated maximum generation. The *standardized* BTM PV generation is obtained by scaling the available capacity into 1 kW, which indicates the trend of solar generation in the LEM area over the day. While the ground-truth PV capacity (G_{max}) of each prosumer is unavailable for the LEM agent. This *standardized* information could also be altered with other data such as weather features, location, panel information, observable PV generation, sky images, etc., if available to the agent.

For each prosumer $i \in I$ at time $t \in H$ on all available days D, find the minimal netload value $nl^-(t)$:

$$nl_i^-(t) = \min_{d \in D, t \in H} nl_i(d,t) \tag{15}$$

The minimal netload set is obtained as:

$$\mathbf{nl_i}^- = [nl_i^-(1), nl_i^-(2), \ldots, nl_i^-(H)] \tag{16}$$

Then the $\mathbf{nl_i}^-$ reflects the netload when the maximum difference between the gross load and BTM PV generation occurs. However, individual $\mathbf{nl_i}^-$ does not necessarily imply same results for other prosumers in the LEM. The maximum generation day d^+ is calculated by matching $\mathbf{nl_i}^-$ with the netload curves in D by finding the minimal error. Without loss of generality, d^+ is determined via a majority voting among all prosumers $\mathcal{N}_p$. After determining the maximum generation day d^+, the minimal hourly nocturnal netload data (i.e., gross load without solar generation) on d^+ is used as the power consumption floor and consumption noise ε. The hypothesis from [33] is that if the BTM PV generation is near its maximum potential (e.g., clear sky generation) and the energy consumption is low (e.g., when a house is unoccupied or no human activities), the best fit lower bound could be estimated by a few data points. By subtracting the power consumption floor and consumption noise ε from the minimal netload set $\mathbf{nl_i}^-$, the maximum BTM PV generation can be estimated after denoising using a Lowess (i.e., locally weighted scatter plot smooth) method to get a smooth output curve of clear-sky solar generation. After obtaining the maximum generation capacity of each prosumer $G_{max.i}$ and the *standardized* PV generation fraction p_{std}, the BTM generation p_i could be estimated using (14). The Mean Absolute Percent Error (MAPE) is leveraged to evaluate the accuracy of the proposed disaggregation method.

$$MAPE = \frac{1}{n} \sum_{k=1}^{n} \left| \frac{\hat{y}_k - y_k}{y_k} \right| \tag{17}$$

where $\hat{y}_k$ and y_k denote the estimated and ground-truth output, respectively, and n denotes the length of time. A lower MAPE indicates a higher accuracy in disaggregation. The calculation is based on gross load desegregation due to MAPE's intolerance to zero PV generation.

IV. Case Studies

To evaluate the effectiveness of the proposed LEM, the following scenarios are selected for comparison: (i) *Baseline:* represents the scenario with ToU and FiT prices adopted in [8]. (ii) *SP:* represents the scenario with single (uniform) hourly price design, which is developed from [7], and (iii) *CP:* represents the scenario with customized hourly price design. It is important to note that the focus of this paper is not to develop the most accurate netload forecasting and BTM PV disaggregation methods. Other cost functions, ToU/FiT prices, load/PV datasets, forecasting models, BTM PV disaggregation methods, and ES parameters are also compatible with the proposed framework.

A. Experiment Setup

The developed LEM is evaluated with a case study containing 10 customers (7 prosumers with PV panels and 3 pure consumers) in Austin, Texas.[2] The netload with a 1-hour resolution over 12 months from January 2018 until December 2018, is selected in our case studies. The ground-truth PV generation is only used for evaluating the disaggregation accuracy. The missing or abnormal data (approximately 5%) is interpolated using neighboring observation.

The LSTM model adopts a deep learning structure with one hidden layer with 200 hidden units, an initial learning rate of 0.005, a dropout rate of 0.2, and the maximum number of epochs of 150. The training algorithm, adaptive moment estimation (Adam), is leveraged to update the training net.

The ToU and FiT price schemes are similar with those in [7], which are also illustrated in Fig. 6(a) as heatmaps. The on-peak hours are 10:00 to 15:00 and 18:00 to 21:00, with a rate of 13.8 ¢/kWh. The flat hours are 7:00 to 10:00, 15:00 to 18:00, and 21:00 to 23:00, with a rate of 8.6 ¢/kWh. The remaining hours are set as off-peak hours with a rate of 3.7 ¢/kWh. The FiT holds a constant rate as 3.5 ¢/kWh for all hours. For the ES parameters, we consider a maximum C_{rate} of 0.5, $SoC \in [0.05, 0.95]$ with an initial minimal value 0.05, and $\eta = 0.95$. The ES capacity is chosen to be 40 kWh in this work.

The netload data of the 10 customers (referred as c1-c10, in which c5, c8, and c10 are pure consumers without BTM PV) and the aggregated netload are shown in Fig. 4(a)–(k). All the prosumers have similar daily diurnal curves with varying capacities due to strong spatial correlations. Besides, the negative netload curves also correspond to different BTM PV installation capacities. It is observed that the profiles have evident various nocturnal patterns, indicating different consumption preferences of customers. Among the 10 customers, c4 and c9 have the highest load level during nocturnal times, with approximately 6 kW. The customers of c1, c6, c7 and c9 have

[2][Online]. Available: https://www.pecanstreet.org/dataport/

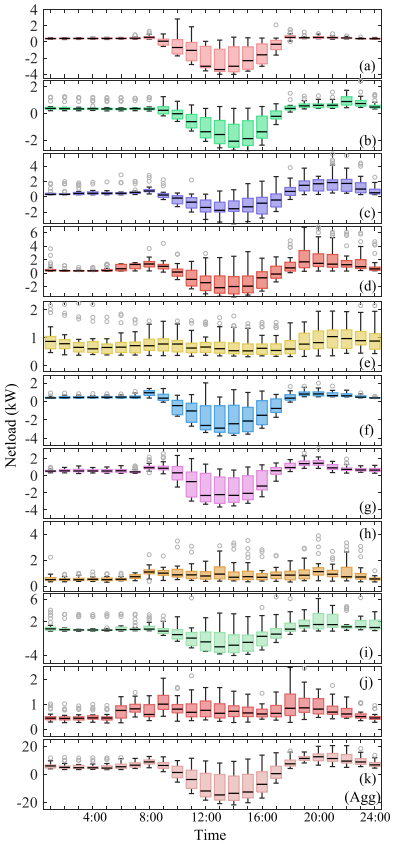

Fig. 4. Hourly statistics of customers' (a)–(k) and aggregated (Agg) netload in January 2018. The box represents the middle 50%, with the median as the black line in the box. The whisker lines indicate the maximum and minimum values of the data. The outliers are illustrated as grey bubbles.

TABLE I
ACCURACY OF NETLOAD DISAGGREGATION, MAPE(%)

c1	c2	c3	c4	c6	c7	c9	Agg
10.12	13.76	19.32	6.38	10.71	12.44	9.53	1.31

the highest negawatt during diurnal periods, with a maximum of approximately −4 kW. Regarding the variability in netload, most customers prefer to consume energy between 20:00 and 24:00, some customers also have morning consumption peaks, while customer 5 has no obvious periodicity compared to other customers. The aggregated netload shows a typical duck curve with negawatt power, which constitutes the motivation of our work.

B. BTM PV Disaggregation Results

Since solar feature time series has strong seasonal patterns, the gross load disaggregation and netload forecasts are generated monthly. Using the estimated maximum generation of each prosumer and standardized PV generation, the BTM PV generation could be extracted, since this step does not require any forecasting information. The netload disaggregation accuracy is summarized in Table I. Due to the variability in netload, the accuracy also varies among different prosumers. It is observed that

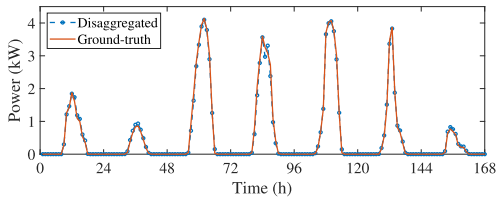

Fig. 5. One-week BTM PV generation of c1 from netload disaggregation.

TABLE II
CORRELATION MATRIX BETWEEN THE AGGREGATED NETLOAD AND NETLOAD OF EACH CUSTOMER

	Agg	c1	c2	c3	c4	c5	c6	c7	c8	c9	c10
Agg	1.0	0.92	0.92	0.84	0.86	0.36	0.94	0.91	0.10	0.86	0.12
c1	0.92	1.0	0.91	0.76	0.73	0.21	0.94	0.91	-0.07	0.74	-0.05
c2	0.92	0.91	1.0	0.77	0.74	0.32	0.91	0.86	-0.01	0.76	0.01
c3	0.84	0.76	0.77	1.0	0.67	0.25	0.78	0.73	0	0.68	-0.01
c4	0.86	0.73	0.74	0.67	1.0	0.34	0.75	0.73	0.08	0.67	0.13
c5	0.36	0.21	0.32	0.25	0.34	1.0	0.27	0.23	0.12	0.28	0.23
c6	0.94	0.94	0.91	0.78	0.75	0.27	1.0	0.91	-0.03	0.75	0.02
c7	0.91	0.91	0.86	0.73	0.73	0.23	0.91	1.0	0.02	0.72	0.05
c8	0.10	-0.07	-0.01	0	0.08	0.12	-0.03	0.12	1.0	0.07	0.25
c9	0.86	0.74	0.76	0.68	0.67	0.28	0.75	0.72	0.01	1.0	0.11
c10	0.12	-0.05	0.01	-0.01	0.13	0.23	0.02	0.05	0.25	0.11	1.0

Note: The high correlation coefficients (>0.9) are marked in colors, and only upper triangular is marked. The grey cells highlight the correlation between three pure consumers.

the aggregated accuracy is better compared with individual disaggregation, due to the high data availability, i.e., ground-truth netload and standardized PV generation. Fig. 5 also presents the BTM PV generation of c1 from netload disaggregation in the first week of January 2018.

C. Netload Forecasting Results

As introduced in Section III-A, the individual netload forecast is generated using the SISO LSTM model, while the aggregated netload forecast is obtained using the MISO LSTM model.

The forecasting setting follows [31] and the data spilt is 0.7/0.2/0.1. The last day of testing set is used to evaluate the LEM performance. Compared with [31], a modification is made in our work; instead of feeding all households' netload data into MISO LSTM, we just pick out the most correlated ones. A Pearson correlation matrix based on the training data is shown in Table II. It is seen that the aggregated netload and some prosumers' netload are highly correlated. Besides, there also exist some strong correlations between some prosumers due to highly correlated BTM PV generations and similar weather features. However, the correlations between pure consumers 5, 8, and 10 are relatively weak, indicating various consumption preferences of consumers. This observation also holds to individual prosumers' gross load.

Though the forecasting model is capable of generating forecasts at multiple forecasting horizons, only 1-day-ahead (1DA) and 1-hour-ahead (1HA) load forecasts are generated in this study. The forecasting results are summarized in Table III. Generally, 1HA forecasting outperforms 1DA forecasting at individual levels, thus it is better to design the real-time customized prices using 1HA data. Similarly, considering member

TABLE III
FORECASTING ERRORS [%] SUMMARY

Customer	c1	c2	c3	c4	c5
nRMSE-1DA	15.96	13.36	17.25	18.74	40.47
nRMSE-1HA	7.58	6.64	14.39	11.43	24.63
Customer	c6	c7	c8	c9	c10
nRMSE-1DA	17.36	16.07	29.93	18.29	28.36
nRMSE-1HA	7.29	8.54	14.29	9.75	18.40
Agg nRMSE-w/o			**17.78**		6.91
Agg nRMSE-w-1			29.53		7.26
Agg nRMSE-w-2		1DA	28.59	1HA	6.55
Agg nRMSE-w-4			24.99		**5.94**
Agg nRMSE-w-6			26.88		7.57

Note: w/o refers to the case of SISO, w-x refers to the case of MISO, and x is the number of extra customers' data as multi-inputs (ranking in descending order by correlation coefficients).

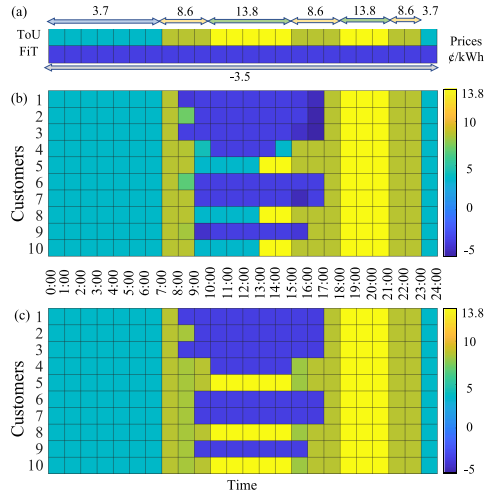

Fig. 6. The customized energy sharing prices of 10 customers on Jan 31. (a) ToU/FiT price, (b) customized price (CP), and (c) single uniform price (SP). The x-axis denotes the time, and y-axis represents price schemes for different customers. The color stands for the price (¢/kWh). Positive values denote the internal selling prices designed for buyers, and negative values denote solar buy-back rates for sellers within the LEM.

customers' time series as additional inputs in the MISO-LSTM could also improve the 1HA forecasting accuracy. We have found that adding 4 extra customers' data with the highest correlation yields the best performance for 1HA aggregated netload forecasting. However, for 1DA aggregated forecasting, since the aggregated level is more predictable, adding extra individual inputs may cause over-fitting problems. This observation also validates the results in [31]. Thus the look-ahead ES capacity scheduling will be determined using 1DA aggregated netload forecasting.

D. Market Performance

1) Price Schemes: Fig. 6(a) shows the ToU/FiT price schemes; Fig. 6(b) and 6(c) present CP and SP design for the 10 customers, respectively. Positive values denote the internal selling prices designed for buyers, and negative values denote solar buy-back rate for sellers within the LEM.

TABLE IV
UTILITIES ($) OF CUSTOMERS AND BENEFIT ($) OF THE AGENT, JAN 31, 2018

Customers' Utility ($)							
	CP	*SP*	*Baseline*		*CP*	*SP*	*Baseline*
c1	4.3695	4.3541	4.3531	c6	5.3813	5.3782	5.3766
c2	3.92558	3.9187	3.9182	c7	8.8368	8.8162	8.8152
c3	4.7803	4.7557	4.7549	c8	12.6109	12.3000	12.2943
c4	25.1207	22.8676	22.8623	c9	14.7221	14.7091	14.7065
c5	4.8512	4.6530	4.6494	c10	9.3840	8.9681	8.9624
Agent's Profit ($)							
Baseline w/ forecasting: 3.3439				*Baseline* w/ ground-truth: 4.1889			
SP w/ forecasting: 4.6783				*SP* w/ ground-truth: 6.1727			
CP w/ forecasting: 9.4534				*CP* w/ ground-truth: 10.8574			

The infeasible range of the internal designed prices is [−3.5, 3.7] ¢/kWh, i.e., buy-back rates lower than FiT and selling rates higher than ToU are unacceptable for customers. Otherwise, the customers may switch to other retail agents or directly trade with the external utility grid. During 0:00–8:00 and 17:00–24:00, the internal price is same with the utility ToU/FiT price due to no/low BTM PV generation. The price transition from positive to negative values indicates the role of the customer is changed, from buyers to sellers, and vice versa.

The LEM agent designs different customized pricing schemes to encourage customers to participate in energy sharing, thereby maximizing its profit with the assistance of ES. By comparing Fig. 6(a)–(c), there exists a potential price discrimination with CP in the LEM, since each customer's flexibility in the energy sharing is different. It is observed from Fig. 6(b) that, the CP design varies for different customers at each hour during 8:00–15:00. For example, the customers of c2, c6, and c9 are offered better selling rates lower than ToU during 8:00–9:00, and c9 is offered a better buy-back rate in the next hour. C4 only acts as a seller during 10:00–14:00, with the shortest time internal among all prosumers, which also corresponds with the netload data shown in Fig. 4(d). As a result, during 9:00–10:00 and 14:00–15:00, c4 is offered significantly better rates compared with the ToU price due to its higher sharing flexibility. In 15:00–16:00, c3 and c7 are offered higher buy-back rates, and c1, c2, and c3 are offered higher rates in the next hour.

It is seen from Fig. 6(c) that with the SP design, the hourly buy-back rate is identical to all sellers in each hour, and similarly, a unique selling price also applies to all buyers. Most sellers are offered with selling prices that are same with FiT, since their excess energy has to be sold due to higher PV generation and lower consumption; otherwise, the excess energy has to be curtailed. In the SP price design case, not all customers' sharing elasticity and DR are fully utilized, while the CP case could promote the customers' energy management and help achieve a higher profit for the LEM agent.

2) Economical Analysis: Table IV summarizes the 10 customers' utilities and the agent's profit under the two pricing schemes and the baseline. The grey color highlights the pure consumers without PV panels. Compared with the baseline, both CP and SP cases yield higher utilities. As the result shows, CP significantly increases the LEM agent's profit without reducing

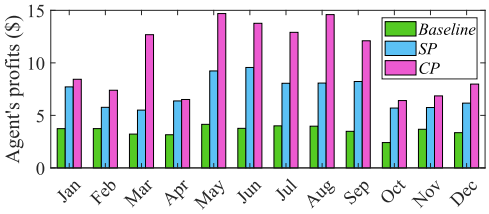

Fig. 7. The LEM agent's profit in the last day of each month (Jan 1st is selected to differ from the aforementioned case).

customers' consumption satisfaction. Since the agent monopolizes the LEM and collects most of the benefits, the proposed LEM design framework is beneficial for the agent to sustain. Besides, most customers are seen to have slightly higher utilities with the CP design scenario. Among all customers, c4 earns the highest increase in the utility due to higher flexibility and received offer in the CP design, as shown in Figs. 4(d) and 6(b). Although accurate forecasting is desired in system operations, the errors are still unavoidable even with state-of-the-art forecasting models. However, the errors could be mitigated through multi-timescale decision-making, where real-time observation of the market and other useful datasets could be incorporated to update the agent's future decision-making. Also, even with the perfect forecasting information, i.e., ground-truth data of customers, the agent is expected to earn a higher profit, as shown in Table IV. Compared with the SP design, it is seen that the CP design is more beneficial for the LEM agent, no matter either forecasting model or ground-truth data is applied. For consumers, since they are always short of electricity and have to purchase energy from others, their market power is relatively low. Similarly, for some excess prosumers, they also have low market power and have to sell their energy, otherwise the surplus energy will be curtailed. While for self-sufficient prosumers, such as c4, the CP case benefits them the most due to their higher sharing flexibility.

In addition to aforementioned cases, a monthly analysis is performed to evaluate the LEM, as shown in Fig. 7. The last day in each month (except Jan., Jan. 1st is selected to differ from the aforementioned case) is selected to calculate the LEM agent's profit. The weather conditions in these 12 days are divided into 3 categories: i) clear-sky, including Mar., May, Jun., and Aug., ii) partially-clear, including Feb., Jul., and Sep., and iii) cloudy, including the remaining months Jan. 1st, Apr., Oct., Nov., and Dec. As seen from the figure, when the local community has more solar generation (i.e., clear-sky and partially-clear days), the CP design significantly outperforms SP. Even if there is no excess negawatt energy for sharing, the LEM agent with the SP case still earns higher profits by fully incentivizing customers' sharing flexibility with ES arbitraging. For example, CP further improves the LEM agent's profit by 4% on Apr 30, when there is almost no energy sharing due to cloudy weather condition and high load demand. While on Mar. 31, the profit percentage increase rises up to 130% due to sunny weather condition and low demand. The LEM welfare is expected to be further

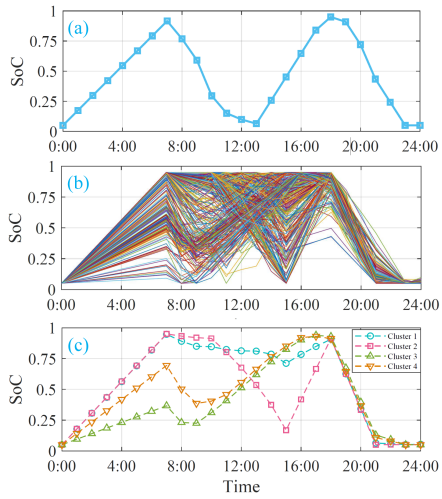

Fig. 8. State of Charge (SoC) of the ES. (a) Jan. 31, (b) 365 days, (c) K-means clustering of 365 days, $K = 4$.

promoted with the increase of market participants, ES capacity, and BTM PV installation. To extend the proposed framework to a large market consisting of thousands of consumers, clustering methods could be leveraged to group the consumers with similar consumption preferences, which has been explored in Refs. [29], [34].

E. ES Profiles

The SoC profile of ES is shown in Fig. 8. More specifically, Fig. 8(a) shows the SoC profile on Jan. 31, (b) shows the profiles throughout the year 2018, and (c) shows the K-means clustering ($K = 4$) result of year 2018.

As seen from the figures, from 0:00 to 7:00 (off-peak hours) and 18:00 to 21:00 (on peak hours), the ES works in a similar pattern in all four clusters. The ES will arbitrage from the utility grid during morning off-peak hours until 7:00, and release stored energy until night on-peak period ends. For Cluster 1, the ES mainly works in a straightforward way, i.e., buffering energy for night on-peak hours. Cluster 2 works similarly in an arbitraging mode, buffering energy in low price periods and discharging in on-peak hours. The difference between Clusters 1 and 2 is that Cluster 1 has no incentive to discharge too much of its stored energy in the afternoon due to sufficient PV generation, while Cluster 2 has to discharge due to limited surplus energy to be shared. Clusters 3 and 4 work in a similar mode while only varying in amount, i.e., arbitraging in the morning off-peak hours, then discharging part of its stored energy in morning flat hours. Thereafter, the ES fully charges again with the excess solar generation from excess prosumers, arbitrages before night on-peak starts, and then discharges in night peak hours until reaching its minimal capacity.

F. Scalability Analysis

Our LSTM forecasting simulations were conducted on a workstation with an Intel Xeon E5-2603 2.50 GHz CPU,

TABLE V
COMPUTATIONAL TIME WITH DIFFERENT NUMBERS OF CONSUMERS

Number of consumers	10	50	100	200
Computation time (s)	4.04	6.90	9.97	20.32

16.0 GB RAM, and an NVIDIA TITAN V GPU. The LSTM forecasting is implemented in MATLAB2020b using deep learning Toolbox, and it takes about 25 seconds to obtain the aggregated netload forecasts, which is applicable for look-ahead ES scheduling. Market simulations were executed on a laptop with an Intel Core i7-6600 U 2.8 GHz CPU and 16.0 GB RAM. At the RT pricing stage, the model works in a centralized manner, and the LEM agent only needs to forecast the 1HA netload for each customer.

To extend the proposed framework to a large market consisting of thousands of customers, clustering methods could be leveraged to group the consumers with similar load patterns, which has been explored in Refs. [29], [34]. In this section, additional case studies with more customers are conducted to show the scalability of our proposed method. Due to limited data availability, extra customer' netload data is generated by multiplying a random factor ranging from 0.5 to 1.5 using the current dataset. The computational cost of real-time pricing is summarized in Table V. It is found that even with 200 customers, the computation cost is approximately 20 seconds, which is acceptable in the (1HA) RT LEM operation, since only the customers who consent to higher flexibility will be selected to be provided with customized incentives. However, too many rates option will compromise the market efficiency, which is not practical in realistic market operation, thus it is more reasonable to design limited options for customer groups.

V. CONCLUSION

This paper proposed a customized price design scheme to address challenges in excess behind-the-meter (BTM) PV generation and energy trading in a local electricity market (LEM). A two-step decision-making strategy was developed, including look-ahead energy storage (ES) scheduling and real-time customized prices design. The impacts of aggregated/individual netload forecasting and BTM disaggregation on LEM were also explored. The results of a case study with 10 customers showed that compared with the single uniform pricing strategy, the customized prices could increase the LEM agent's profit by 4% to 130%, while also maintaining the customers' consumption satisfaction.

The proposed LEM with customized pricing strategies could be further extended in multiple directions. First, the proposed LEM could be readily applied with other netload/solar forecasting models or disaggregation methods. Second, the dataset in the current study only contains the aggregated netload in the household. If customers' appliance identification could be obtained, more accurate forecasts could be generated for the LEM price design. Third, other entities and market schemes could also be considered in the LEM, such as distributed energy resources owners, third-party owned energy storage, market bidding stakeholders, and cooperative trading mode. Lastly, another direction is privacy-preserving LEM design. Approaches such as private structure and pricing method, game theory, blockchain, distributed algorithm, federated learning, etc., could be potentially leveraged for promoting information security and privacy in LEM.

REFERENCES

[1] W. Tushar et al., "Challenges and prospects for negawatt trading in light of recent technological developments," *Nature Energy*, vol. 5, no. 11, pp. 834–841, 2020.
[2] D. Feldman, A. M. Brockway, E. Ulrich, and R. Margolis, "Shared solar. Current landscape, market potential, and the impact of federal securities regulation," Nat. Renewable Energy Lab., Golden, CO, USA, *Tech. Rep.*NREL/TP-6A20-63892, 2015.
[3] L. He and J. Zhang, "A community sharing market with PV and energy storage: An adaptive bidding-based double-side auction mechanism," *IEEE Trans. Smart Grid*, vol. 12, no. 3, pp. 2450–2461, May 2021.
[4] C. Zhang, J. Wu, Y. Zhou, M. Cheng, and C. Long, "Peer-to-peer energy trading in a microgrid," *Appl. Energy*, vol. 220, pp. 1–12, 2018.
[5] N. Liu, L. He, X. Yu, and L. Ma, "Multiparty energy management for grid-connected microgrids with heat- and electricity-coupled demand response," *IEEE Trans. Ind. Informat.*, vol. 14, no. 5, pp. 1887–1897, May 2018.
[6] W. Tushar et al., "Energy storage sharing in smart grid: A modified auction-based approach," *IEEE Trans. Smart Grid*, vol. 7, no. 3, pp. 1462–1475, May 2016.
[7] N. Liu, M. Cheng, X. Yu, J. Zhong, and J. Lei, "Energy sharing provider for PV prosumer clusters: A hybrid approach using stochastic programming and Stackelberg game," *IEEE Trans. Ind. Electron.*, vol. 65, no. 8, pp. 6740–6750, Aug. 2018.
[8] L. He and J. Zhang, "Distributed solar energy sharing within connected communities: A coalition game approach," in *Proc. IEEE Power Energy Soc. Gen. Meeting*, 2019, pp. 1–5.
[9] A. Fleischhacker, H. Auer, G. Lettner, and A. Botterud, "Sharing solar PV and energy storage in apartment buildings: Resource allocation and pricing," *IEEE Trans. Smart Grid*, vol. 10, no. 4, pp. 3963–3973, Jul. 2019.
[10] D. Kalathil, C. Wu, K. Poolla, and P. Varaiya, "The sharing economy for the electricity storage," *IEEE Trans. Smart Grid*, vol. 10, no. 1, pp. 556–567, Jan. 2019.
[11] A. Paudel, K. Chaudhari, C. Long, and H. B. Gooi, "Peer-to-peer energy trading in a prosumer-based community microgrid: A game-theoretic model," *IEEE Trans. Ind. Electron.*, vol. 66, no. 8, pp. 6087–6097, Aug. 2019.
[12] M. Khorasany, Y. Mishra, and G. Ledwich, "Market framework for local energy trading: A review of potential designs and market clearing approaches," *IET Gener., Transmiss. Distrib.*, vol. 12, no. 22, pp. 5899–5908, 2018.
[13] J. M. Arroyo and A. J. Conejo, "Multiperiod auction for a pool-based electricity market," *IEEE Trans. Power Syst.*, vol. 17, no. 4, pp. 1225–1231, Nov. 2002.
[14] K. Chen, J. Lin, and Y. Song, "Trading strategy optimization for a prosumer in continuous double auction-based peer-to-peer market: A prediction-integration model," *Appl. Energy*, vol. 242, pp. 1121–1133, 2019.
[15] J. Guerrero, A. C. Chapman, and G. Verbič, "Decentralized P2P energy trading under network constraints in a low-voltage network," *IEEE Trans. Smart Grid*, vol. 10, no. 5, pp. 5163–5173, Sep. 2019.
[16] L. He, Y. Liu, and J. Zhang, "Peer-to-peer energy sharing with battery storage: Energy pawn in the smart grid," *Appl. Energy*, vol. 297, 2021, Art. no. 117129.
[17] X. Kong, D. Kong, J. Yao, L. Bai, and J. Xiao, "Online pricing of demand response based on long short-term memory and reinforcement learning," *Appl. Energy*, vol. 271, 2020, Art. no. 114945.
[18] Y. Zong, D. Kullmann, A. Thavlov, O. Gehrke, and H. W. Bindner, "Application of model predictive control for active load management in a distributed power system with high wind penetration," *IEEE Trans. Smart Grid*, vol. 3, no. 2, pp. 1055–1062, Jun. 2012.
[19] P. Shamsi, H. Xie, A. Longe, and J.-Y. Joo, "Economic dispatch for an agent-based community microgrid," *IEEE Trans. Smart Grid*, vol. 7, no. 5, pp. 2317–2324, Sep. 2016.

[20] W. Tushar, C. Yuen, D. B. Smith, and H. V. Poor, "Price discrimination for energy trading in smart grid: A game theoretic approach," *IEEE Trans. Smart Grid*, vol. 8, no. 4, pp. 1790–1801, Jul. 2017.
[21] T. D. Couture, K. Cory, C. Kreycik, and E. Williams, "Policymaker's guide to feed-in tariff policy design," Nat. Renewable Energy Lab., Golden, CO, USA, *Tech. Rep.*NREL/TP-6A2-44849, 2010.
[22] C. Long, J. Wu, Y. Zhou, and N. Jenkins, "Peer-to-peer energy sharing through a two-stage aggregated battery control in a community microgrid," *Appl. Energy*, vol. 226, pp. 261–276, 2018.
[23] X. Fang, B.-M. Hodge, L. Bai, H. Cui, and F. Li, "Mean-variance optimization-based energy storage scheduling considering day-ahead and real-time LMP uncertainties," *IEEE Trans. Power Syst.*, vol. 33, no. 6, pp. 7292–7295, Nov. 2018.
[24] R. Lu, T. Ding, B. Qin, J. Ma, X. Fang, and Z. Dong, "Multi-stage stochastic programming to joint economic dispatch for energy and reserve with uncertain renewable energy," *IEEE Trans. Sustain. Energy*, vol. 11, no. 3, pp. 1140–1151, Jul. 2020.
[25] L. He and J. Zhang, "Customized prices design for agent-based local energy market with PV and energy storage," in *Proc. IEEE North Amer. Power Symp.*, 2021, pp. 1–6.
[26] N. Liu, X. Yu, C. Wang, C. Li, L. Ma, and J. Lei, "Energy-sharing model with price-based demand response for microgrids of peer-to-peer prosumers," *IEEE Trans. Power Syst.*, vol. 32, no. 5, pp. 3569–3583, Sep. 2017.
[27] J. Saez-Gallego, J. M. Morales, M. Zugno, and H. Madsen, "A data-driven bidding model for a cluster of price-responsive consumers of electricity," *IEEE Trans. Power Syst.*, vol. 31, no. 6, pp. 5001–5011, Nov. 2016.
[28] O. Corradi, H. Ochsenfeld, H. Madsen, and P. Pinson, "Controlling electricity consumption by forecasting its response to varying prices," *IEEE Trans. Power Syst.*, vol. 28, no. 1, pp. 421–429, Feb. 2013.
[29] C. Feng, Y. Wang, K. Zheng, and Q. Chen, "Smart meter data-driven customizing price design for retailers," *IEEE Trans. Smart Grid*, vol. 11, no. 3, pp. 2043–2054, May 2020.
[30] W. Kong, Z. Y. Dong, Y. Jia, D. J. Hill, Y. Xu, and Y. Zhang, "Short-term residential load forecasting based on LSTM recurrent neural network," *IEEE Trans. Smart Grid*, vol. 10, no. 1, pp. 841–851, Jan. 2019.
[31] S. E. Razavi, A. Arefi, G. Ledwich, G. Nourbakhsh, D. B. Smith, and M. Minakshi, "From load to net energy forecasting: Short-term residential forecasting for the blend of load and PV behind the meter," *IEEE Access*, vol. 8, pp. 224343–224353, 2020.
[32] K. Li, F. Wang, Z. Mi, M. Fotuhi-Firuzabad, N. Duić, and T. Wang, "Capacity and output power estimation approach of individual behind-the-meter distributed photovoltaic system for demand response baseline estimation," *Appl. Energy*, vol. 253, 2019, Art. no. 113595.
[33] D. Chen and D. Irwin, "SunDance: Black-box behind-the-meter solar disaggregation," in *Proc. 8th Int. Conf. Future Energy Syst.*, 2017, pp. 45–55.
[34] J. Yang, J. Zhao, F. Wen, and Z. Y. Dong, "A framework of customizing electricity retail prices," *IEEE Trans. Power Syst.*, vol. 33, no. 3, pp. 2415–2428, May 2018.

Li He (Member, IEEE) received the B.S. and M.S. degrees in electrical engineering from North China Electric Power University, Beijing, China, in 2015 and 2018, respectively, and the Ph.D. degree in electrical engineering from the Department of Electrical and Computer Engineering, The University of Texas at Dallas, Richardson, TX, USA, in 2022. His research interests include transactive energy, demand response, game theory, renewable integration, and energy management.

Jie Zhang (Senior Member, IEEE) received the B.S. and M.S. degrees in mechanical engineering from the Huazhong University of Science and Technology, Wuhan, China, in 2006 and 2008, respectively, and the Ph.D. degree in mechanical engineering from Rensselaer Polytechnic Institute, Troy, NY, USA, in 2012. He is currently an Associate Professor with the Department of Mechanical Engineering and (Affiliated) Department of Electrical and Computer Engineering, The University of Texas at Dallas, Richardson, TX, USA. His research interests include integrated energy systems, renewable energy grid integration, complex networks, big data analytics, and multidisciplinary design optimization.